

## Nichols stability analysis in multiwall carbon nanotube based interconnects

Somayeh Fotoohi<sup>1\*</sup>, Saeed Haji-Nasiri<sup>2</sup>

<sup>1</sup>Department of Electrical Engineering, Islamshahr Branch, Islamic Azad University, Tehran, Iran

<sup>2</sup>Department of Electrical, Biomedical, and Mechatronics Engineering, Qazvin Branch, Islamic Azad University, Qazvin 3419915195, Iran

Received June 26, 2015, Revised September 10, 2015

We present Nichols stability analysis based on transmission line modeling for multiwall carbon nanotube (MWCNT) interconnects. This is the first instance that such an analysis has been presented for MWCNT so far. In this analysis, dependence of the degree of relative Nichols stability for MWCNT interconnects on the geometry of each tube has been acquired. It is shown that with increasing the length and the diameter of each tube, MWCNT interconnects become more stable.

**Keywords:** Multiwall carbon nanotube, interconnects, Nichols stability, phase and gain margin.

### BACKGROUND

Quoting the International Technology Roadmap for Semiconductors (ITRS) report: “traditional interconnect scaling will no longer satisfy performance requirements.

Defining and finding solutions beyond copper will require material innovation, combined with accelerated design, packaging and unconventional interconnect.” The main challenges in scaling Cu interconnects are given by the poor current density allowed and the steep increase of the resistivity. Furthermore, the current density required for such technologies will rise to values well beyond the maximum allowed for copper. For these reasons, metallic CNTs have been suggested to replace copper in nano-interconnects [1].

CNTs have long mean free paths (MFPs) on the order of several micrometers (as compared to 40 nm for Cu at room temperature), which provide low resistivity and possible ballistic transport in short-length interconnects. More importantly, an isolated CNT can carry current densities in excess of 1010 A/cm<sup>2</sup> without any signs of damage even at an elevated temperature of 250°C, thereby eliminating electromigration reliability concerns that plague nanoscale Cu interconnects [2].

While CNTs have desirable material properties, individual nanotubes suffer from an intrinsic ballistic resistance of approximately 6.5 k that is not dependent on the length of the nanotube. To reduce the impact of the resistance of individual nanotubes, bundles of CNTs in parallel, which have

been proposed as a medium for, interconnect in very large scale integration (VLSI) applications [3]. Fig. 1 illustrates a schematic representation of a typical RLC model for a MWCNT interconnect made of N CNTs of the same lengths  $l$  and out-diameters  $D$ . In this figure,  $R_C$ ,  $R_Q$ , and  $R_S$  represent the equivalent resistances introduced by the imperfect contacts, the quantum effect, and the carriers’ scatterings, respectively. One can approximate the quantum contact resistance as  $R_Q \approx h \{2e^2 N_{ch} N\}^{-1}$  [4], wherein  $h$ ,  $e$ , and  $N_{ch}$  are the Plank’s constant, electron charge, and number of conducting channels in each CNT. When the length of each CNT is greater than its carriers’ mean free path ( $\lambda$ ), the equivalent distributed ohmic resistance (per unit length) introduced by carriers scatterings with defects, substrate-induced disorders, and phonons can be written as  $R_S \equiv R_Q / \lambda$  [4]. Also shown in Fig. 1  $C_E \approx 2\pi\epsilon / (N \times \ln(y/D))$  [5] in which  $\epsilon$  is the dielectric permittivity,  $y$  is distance of MWCNT from ground plane, and  $D$  is diameter of each tube.  $C_Q \approx \{R_Q v_F\}^{-1}$  is the per unit length values of the equivalent capacitances induced by the electrostatic and quantum effects, respectively, in which  $v_F$  is the Fermi velocity in graphite.

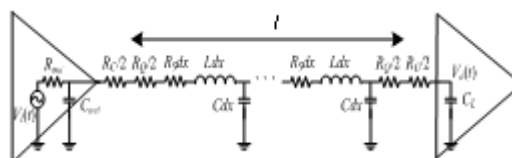


**Fig. 1.** Simple RLC schematic of transmission line circuit model for a driver- MWCNT interconnect-load configuration.

\*To whom all correspondence should be sent:  
E-mail: somayehfotoohi@yahoo.com

Since the separation between any two CNT is much smaller than  $y$ , the effect of the electrostatic capacitances between any two CNT in the bundle is negligible. Furthermore,  $L_K=R_Q/v_F$  and  $L_M \approx \mu \times \ln(y/D)/(2\pi N)$  [5] represent the per unit length values of the kinetic and the magnetic inductances, in presence of the ground plane, wherein  $\mu$  is the CNT permeability. In a practical case  $L_M \ll L_K$  [4].

In order to obtain the number of conducting channels in each CNT, one can add up contributions from all electrons in all  $n_C$  conduction sub-bands and all holes in all  $n_V$  valence sub-bands [6]:

$$N_{ch} = \sum_{i=1}^{n_C} \left[ e^{(E_i - E_F)/kT} + 1 \right]^{-1} + \sum_{i=1}^{n_V} \left[ e^{(E_i + E_F)/kT} + 1 \right]^{-1}, \quad (1)$$

where  $i(=1, 2, 3, \dots)$  is a positive integer,  $E_F$ ,  $k$ , and  $T$  are the Fermi energy, the Boltzmann constant, and temperature, respectively, and  $E_i$  represents the quantized energy that corresponds to the  $i$ -th conduction or valence sub-band. This quantization is due to diameter confinement, introduced by the tube's finite diameter.

In spite of the valuable properties there are several prospect that must be investigated to practical use of carbon nanotube interconnects. Stability analysis in driver-carbon nanotube interconnect-load system is an important viewpoint in performance evaluation of this system. In this paper we have used Nichols analysis as a criterion to compare the relative stability by changing the geometry of the CNTs. Before the frequency response analysis using Nichols chart, we need to ask the following questions:

What is the difference between Nichols chart and any other analysis method like bode and Nyquist plot? What is the advantage of using it?

A Nichol plot is similar to a Nyquist plot but shows gain on a logarithmic scale (dB) vs. phase on a linear scale (degrees), with an axis origin at the point (0dB, -180°). The advantage of Nichol's chart is the ease by which gain and phase margins can be determined graphically. The gain margin (GM) is the vertical distance in dB measured from the phase crossover to the critical point (the phase crossover frequency is where the locus intersects the -180 axis). The phase margin (PM) is the horizontal distance measured in degrees from the gain crossover to the critical point (the gain crossover frequency is where the locus intersects the 0 dB). The system becomes more stable if the GM and PM increase [7].

## MATRIX FORMULATION

In the configuration illustrated in Fig. 1, a MWCNT interconnect of length  $l$  that is represented by a series of distributed resistances ( $R_s$ ), inductances ( $L$ ), and capacitances ( $C$ ) (all in per length units), is driven by a driver with an output resistance  $R_{out}$  and an output capacitance  $C_{out}$ . The MWCNT interconnects is also connected to a load of capacitance  $C_L$ .

In order to calculate the input-output transfer function of the configuration in Fig. 1, total transmission parameter matrix should be derived. For this purpose ABCD transmission parameter matrix are used for a uniform RLC transmission line of length  $l$  that contains  $N_B$  distributed blocks. Accordingly, total ABCD transmission parameter matrix is defined as:

$$T_{total} = \begin{bmatrix} A_T & B_T \\ C_T & D_T \end{bmatrix} \equiv \begin{bmatrix} 1 & R_{out} \\ 0 & 1 \end{bmatrix} \begin{bmatrix} 1 & 0 \\ sC_{out} & 1 \end{bmatrix} \begin{bmatrix} 1 & R_{in} \\ 0 & 1 \end{bmatrix} \times \left[ \begin{array}{cc} 1 + (R_s dx + L dx s) s C dx & (R_s dx + L dx s) \\ s C dx & 1 \end{array} \right]^{N_B} \times \begin{bmatrix} 1 & R_{in} \\ 0 & 1 \end{bmatrix}, \quad (2)$$

Where  $R_{ex}=(R_C+R_Q)/2$ ,  $L=L_K+L_M$ ,  $C=C_E C_Q/(C_E+C_Q)$ ,  $dx=l/N_B$ , and  $s=j\omega$  is the complex frequency. We obtain the linear parametric equivalent for the transfer function of as:

$$H(s) = \frac{V_o(s)}{V_i(s)} = \frac{1}{A_T + s C_T B_T}, \quad (3)$$

### Nichols stability analysis

By varying the nanotubes' dimensions, ( $2 \mu m \leq l \leq 10 \mu m$  and  $2 \text{ nm} \leq D \leq 10 \text{ nm}$ ) and generating various Nichols diagrams, we have studied the effect of MWCNT geometry on the relative stability of the configuration given in Fig. 1. All geometrical and physical parameters are according to the 22-nm technology node, extracted from ITRS2009 [8]. Both local interconnects are assumed to have ideal contact (i.e.,  $R_C=0$ ) [8]. The driver size is set to be 100 times the minimum sized gate for the 22-nm technology node, given in [8]. The bundle width is 22 nm and its thickness is 44 nm. The space between two adjacent CNTs is assumed as 0.34 nm and  $E_F$  as 0.3 eV. All individual CNTs are metallic.

Nichols diagrams are shown in Fig. 2 for the configuration of Fig. 1 regarding  $l=2, 6, \text{ and } 10 \mu m$ .

The diameter of each tube is assumed to be 2 nm. As shown in Fig. 2, by increasing the length of CNTs to 2, 6, 10  $\mu\text{m}$ , the curves in the critical point shift to the down and right, consequently the gain margin of interconnect increases as 0.54, 2.34 and 4.13, and the phase margin of interconnect increases as -4.64, 44 and 133 respectively.

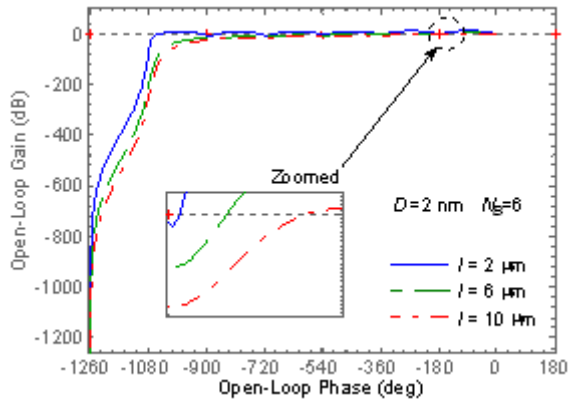


**Fig. 2.** The Nichols diagrams for driver-MWCNT interconnect-load configuration of Fig. 1 for  $D=2 \text{ nm}$  and  $2 \mu\text{m} \leq l \leq 10 \mu\text{m}$ .

Thus, with an increase in the length of CNT bundle, the system becomes more stable. This is because by increasing the length of tubes, the equivalence impedance of the interconnect increases so that the step response of the system go to more damping and the system tend to be more stable.

Nichols diagrams for  $D = 2, 6,$  and  $10 \text{ nm}$  are illustrated in Fig. 3. The length of each tube is assumed to be  $2 \mu\text{m}$ . As shown in Fig. 3, by increasing the diameter of CNT to 2, 6 and  $10 \text{ nm}$ , the curves in the critical point shift to the down and right, consequently the gain margin of interconnect increases as 0.54, 1.02 and 1.46, and the phase margin of interconnect increases as -4.64, 13.3 and 27 respectively. Therefore, with an increase in the diameter of CNT bundle, the system approaches to more stability. This is because by increasing the tube diameters the bundle becomes less dense and its conductivity decreases so that its step response tends to be more damping.

The present general analysis whose transfer function is of the order of 14, provides much more accurate and realistic numerical results than those that could be obtained by similar analyses presented in [9] with order of four and [10] with the order of six both for CNT-bundle interconnects, and in [11] with the order of four for multi layer graphene nanoribbon (MLG NR) interconnects.

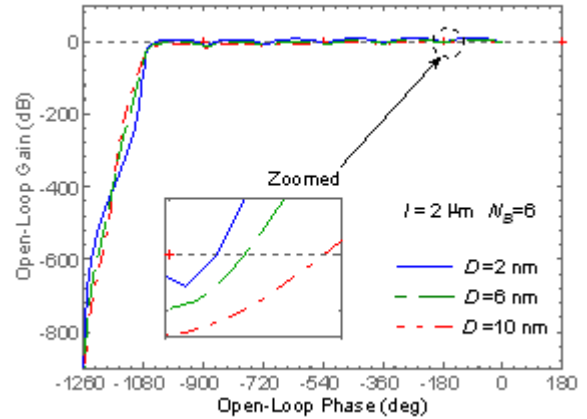


**Fig. 3.** The Nichols diagrams for driver-MWCNT interconnect-load configuration of Fig. 1 for  $l=2 \mu\text{m}$  and  $2 \text{ nm} \leq D \leq 10 \text{ nm}$ .

## CONCLUSION

Using transmission line modeling along with Nichols stability diagrams, relative stability for MWCNT interconnects has been studied. We have shown that with increasing either the length or diameter of each tube, the relative stability increases and hence the system becomes more stable. This is because an increase in either parameter gives rise to switching delay and hence, its step response tends to damp faster and as a result, the system becomes more stable.

## REFERENCES

1. A. Maffucci, G. Miano, F. Villone, *IEEE T. Advanced Packaging*, **21**, 692 (2008).
2. H. Li, W.Y. Yin, K. Banerjee, J.F. Mao, *IEEE Electron Device Lett.*, **55**, 1328 (2008).
3. A. Nieuwoudt, Y. Massoud, *IEEE T. Nanotechnology*, **5**, 758 (2006).
4. N. Srivastava, K. Banerjee, *IEEE ICCAD*, **23**, 38 (2005).
5. H. Hayt, A. Buck, Engineering Electromagnetics, McGraw-Hill, New York, 2005.
6. A. Naemi, D. Meindl, *IEEE Electron Device Lett.* **27**, 338 (2006)
7. R. Dorf, R. Bishop, Modern Control System, Englewood Cliffs, NJ, Prentice-Hall, 2008.
8. International Technology Roadmap for Semiconductors (ITRS),
9. <http://www.itrs.net/Links/2010ITRS/Home2010.htm>.
10. D. Fathi, B. Forouzandeh, *IEEE Electron Device Lett.* **30**, 475 (2009).
11. D. Fathi, B. Forouzandeh, S. Mohajerzadeh, R. Sarvari, *Micro & Nano letters*, **4**, 116 (2009).
12. S. Haji-Nasiri, M. K. Moravvej-Farshi, R. Faez, *IEEE Electron Device Lett.* **31**, 1458 (2010).